

Spatial and chemical interface asymmetry in Fe/MgO/Fe(001) heterostructures

F. J. Palomares^{a)} and C. Munuera

Instituto de Ciencia de Materiales de Madrid (CSIC), Cantoblanco, 28049 Madrid, Spain

C. Martínez Boubeta and A. Cebollada

Instituto de Microelectrónica de Madrid IMM (CNM-CSIC), Isaac Newton 8, P.T.M. 28760 Madrid, Spain

(Received 8 October 2004; accepted 20 November 2004; published online 14 January 2005)

The chemical nature of the different interfaces and possible segregation effects are studied in fully epitaxial Fe/MgO/Fe (001) oriented heterostructures fabricated by combined sputtering plus laser ablation deposition techniques. Auger electron spectroscopy depth profiling experiments showed that the interfaces of the MgO spacer with the Fe layers are different, the inner MgO/Fe being spatially broader and with an FeO interlayer, while that of the outer Fe/MgO is spatially narrower with no evidence of FeO formation. This spatial and chemical asymmetry is interpreted in terms of the different deposition procedures, which affect the formation of both interfaces. No Fe segregation in the MgO layers or MgO segregation in the Fe films is observed. © 2005 American Institute of Physics. [DOI: 10.1063/1.1847718]

In recent years, fully epitaxial magnetic tunnel junctions made out of Fe/MgO/Fe (001) type heterostructures have been the object of study due to the high-predicted values (as high as 6000%) of tunnel magnetoresistance (TMR).^{1,2} Nevertheless, the experimentally measured TMR in this kind of structure is in the range from 15 up to 67% at room temperature (RT).³⁻⁵ A plausible explanation is that, in actual junctions, a number of factors not easy to include in theoretical models such as segregation between different layers, electrode oxidation at the interface with the oxide barrier, or interface asymmetry in nominally symmetric interfaces, can alter the interface nature and consequently the transport properties. In this sense, theoretical calculations have recently shown⁶ that the presence of an FeO layer in the Fe/FeO/MgO/Fe (001) system reduces the TMR ratio with respect to the symmetrical case due to a decrease in the majority channel conductance, approaching the experimentally obtained values.

The presence of such an interfacial FeO layer in MgO/Fe(001) (say “barrier/bottom electrode”) structures has been reported⁷⁻⁹ for MgO high temperature reactive deposition of Mg in the presence of oxygen, an Fe-oxide formation which is thermodynamically favored.¹⁰ Nevertheless, an open question not yet reported is the nature of the Fe/MgO(001) (“top electrode/barrier”) interface, which is nominally symmetric and equivalent to the MgO/Fe, but that in real systems might exhibit different properties. In fact, in the MgO/Fe interface formation, sometimes carried out at high temperatures, the very likely presence of atomic O can favor the oxidation of the Fe(001) surface. Besides, in the case of MgO laser ablation, the energetics intrinsic to the deposition method can give rise to interdiffused interfaces. On the other hand, the Fe/MgO interface formation is usually performed by thermal evaporation or sputtering of Fe at RT on a well-formed, stable MgO(001) surface. Therefore the structure and chemi-

cal nature of the MgO interfaces with top and bottom electrodes does not necessarily need to be the same. The aim of this work is to investigate the nature of both interfaces in complete Fe/MgO/Fe heterostructures, especially in the Fe/MgO case.

Samples ($5 \times 5 \text{ mm}^2$) were fabricated on MgO(001) substrates by combined sputtering and laser ablation deposition techniques, as can be found elsewhere.^{11,12} Chemical analysis of the samples and depth profiling experiments were carried out by Auger electron spectroscopy (AES) in an ultra-high vacuum JEOL-Jamp-10S scanning microscope by ion bombardment. The electron gun was operated at energy of 5 keV, a current of 120 nA, and had a 60- μm -diam spot. Ion etching of the samples was performed with Ar⁺ gun (2 keV, 10 nA current) on a rastered area of $2 \times 2 \text{ mm}^2$, to ensure the signal collection exclusively from the eroded area, and to minimize the number of induced defects and interdiffusion between adjacent layers. For quantitative analysis, KLL (503 eV), LMM (703 eV), and KLL (1174 eV) Auger transitions of O, Fe, and Mg, respectively, were considered. A more detailed description of the technique can be found in Ref. 13. *Ex situ* atomic force microscopy (AFM) measurements were performed in several MgO/Fe heterostructures to study the influence of the MgO deposition temperature on the growth mode and morphology of the barrier.

In this work several samples corresponding to the different steps in the fabrication of the final trilayered Fe/MgO/Fe structure were grown. Once checked the purity of the Fe bottom layers deposited at room temperature and annealed at 670 K on the buffered substrate as well as the correct stoichiometry of the deposited MgO films, with no preferential Mg vs O sputtering observed,¹⁴ we first proceeded to analyze a series of MgO/Fe(001) bilayered structures, where MgO films of different thicknesses (50, 100, 200 Å) were grown at 670 K onto the Fe surface. Upon inspection of the high kinetic energy region in the AES spectra of the as-received samples, a significant Fe LMM signal, besides the O and Mg

^{a)}Electronic mail: fjpalmomares@icmm.csic.es

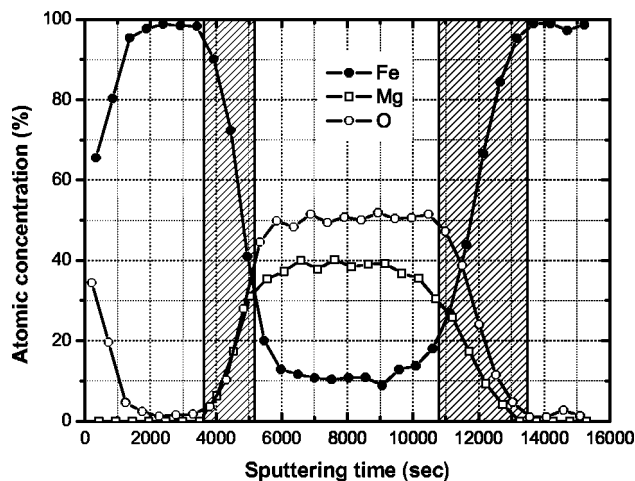


FIG. 1. AES depth profile of a 100 Å Fe(RT)/200 Å MgO(670 K)/500 Å Fe(RT+annealed) trilayered structure where the interface region for the MgO/Fe case is broader than the Fe/MgO one.

peaks from the MgO layer, is observed regardless of the MgO thickness. This can be due to Fe floating on the MgO surface, Fe interdiffusion into the barrier layer, or Fe signal from the bottom electrode due to the presence of pinholes in the MgO layer. Nevertheless, in AES depth profiling experiments of the bilayer, the intensity evolution of Fe, O, and Mg peaks as the MgO ion-milling process proceeds exhibiting constant values, contrary to what should be expected in the case of Fe floating on the MgO or gradual Fe diffusion through the MgO barrier. This means that the barrier grown at this temperature has pinholes and does not cover completely the Fe layer underneath.

As a next step, a set of trilayer Fe/MgO/Fe structures with upper Fe layer 50, 100, and 200 Å thick were fabricated to determine the symmetry of the Fe–MgO vs MgO–Fe interface. MgO spacer deposition was at 670 K and the upper Fe layers were grown at RT. Detailed AES depth profiling characterization was performed in the trilayers to determine the atomic concentration of each element in the heterostructure, and the symmetry and width of the Fe–MgO vs MgO–Fe interfaces. Different thicknesses of the Fe upper electrode were considered to evaluate the effect of the intrinsic interface broadening with depth from the ion-milling process. For the sake of clarity, only the results corresponding to the trilayer with 100 Å Fe upper electrode have been considered for discussion, as shown in Fig. 1. In this case, and after removal of a contaminant layer adsorbed during the transfer in air of the sample, the top Fe layer is detected (between 1500 and 3500 s sputtering) in which neither Mg nor O signals are observed. Between 3500 and 5200 s, the Fe–MgO interface is explored. The Fe concentration decreases, and, correspondently, Mg and O ones increase. The MgO layer has the correct 1:1 stoichiometry, as determined from the sensitivity factors obtained with previous samples, and therefore, there is no O signal left that might contribute to the formation of Fe-oxide. As the ion-milling continues (between 5200 and 10 700 s) a constant Fe signal is clearly observed in the region corresponding to the MgO barrier, a result consistent with the AES depth profiling experiments performed in the MgO/Fe bilayers. In principle, although the

O and Fe atomic percentages observed might suggest the formation of Fe-oxide in the stoichiometric MgO layer due to Fe interdiffusion, it does not account for it, but it is explained in terms of the existence of holes through which the AES technique is able to explore and get information of the first layers in the deeper MgO–Fe interface (see the following). For milling times between 10 700 and 13 500 s, the evolution of the atomic concentration with depth across the MgO/Fe interface shows a decrease of the Mg and O signals, which do not overlap each other as expected for the existence of only stoichiometric MgO. In fact, the difference of both contents remains approximately constant and equals an extra O percentage of 10%, which is attributed to the presence of an Fe-oxide interfacial layer in a near 1:1 Fe:O ratio. Moreover, it is evident that the asymmetric nature of interfaces at each side of the barrier comes from not only the width (being the MgO/Fe broader), but also from the composition and oxidation state (chemically abrupt Fe–MgO vs MgO–FeO–Fe interface). This effect is illustrated in Fig. 1 with shadowed bands of different width at the places where the interfaces are. This wider MgO/Fe interface, together with slightly different decaying rates for the Mg and O signals, probably indicates a dissociation of the Mg–O bond, giving rise to the Fe oxide interfacial layer, as observed by Meyerheim *et al.*^{7,8} and Oh *et al.*⁹ when depositing the MgO layer at high temperature, and justified by Vassent *et al.*¹⁰ according to entropic arguments. The thinner Fe/MgO interface can be due to the deposition of Fe on a well-established, strongly bonded MgO surface, at low deposition temperature. Nevertheless, this behavior could also emphasize the importance of the preparation conditions to form the Fe/MgO/Fe heterostructures since different annealing processes and deposition techniques are used, sputtering and laser ablation, for Fe and MgO, respectively. Likewise, it is worth mentioning that the asymmetry observed at the interfaces is equivalent for the three trilayered structures, regardless of the Fe upper electrode thickness (50, 100, or 200 Å), eradicating the origin as a broadening due to the ion-milling process, in which case the observed width would be larger for the thicker ones.

Taking into account the results obtained from the previous series of samples, three different 200 Å MgO/500 Å Fe bilayers were grown. To study the effect of temperature on the modification of the morphological properties of the barrier in terms of better continuity and the absence of holes, the MgO barriers were deposited at 670 K (sample A), RT (sample B), and RT followed by 670 K thermal treatment for 10 minutes (sample C). Figure 2(a) shows the high kinetic energy AES spectra taken for the three samples previous to ion milling. Carbon and oxygen peaks are visible due to contamination induced by exposure to air when transferring the samples into the AES spectrometer chamber. The three main Fe LMM characteristic transition peaks are clearly observed in sample A, in agreement to what was observed in the set of trilayered samples, while they are very weak for sample B grown at RT, and indistinguishable from the background in sample C with annealed MgO barrier. On the other hand, low energy spectra (not shown) with more sensitivity to the outermost surface layers, reveal the presence of iron oxide features for sample A; samples B and C display low

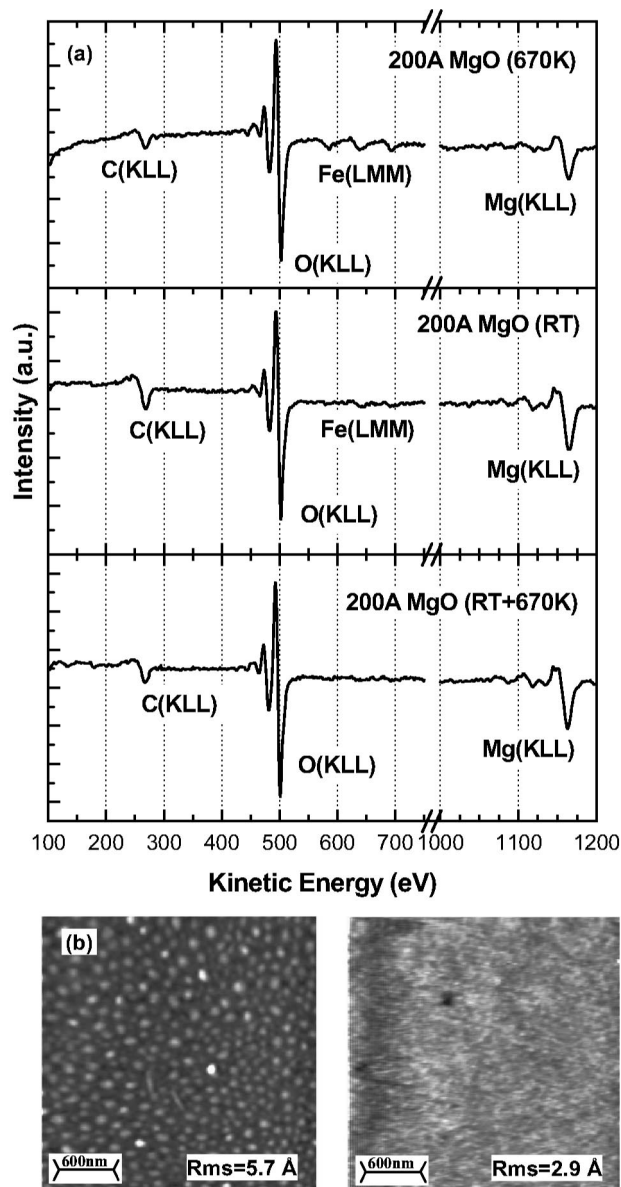


FIG. 2. (a) High kinetic energy AES spectra taken for three 200 Å MgO barriers deposited at 670 K (sample A), RT (sample B), and RT followed by 670 K thermal treatment for 10 min (sample C), on an annealed 500 Å Fe layer. (b) AFM measurements of a MgO surface deposited on a Fe layer at RT (left), and subsequently annealed at 670 K during 10 min (right).

energy features similar to that of the MgO reference layers. From these results it is clear that the different annealing steps induced some changes in the barrier, which might affect its properties somehow.

In order to elucidate whether any morphological modification took place, AFM measurements were carried out in these bilayered structures. The AFM images in Fig. 2(b) evidence the presence of holes in MgO layers deposited at 670

K and RT. In contrast, for the MgO layer deposited at RT and annealed, no holes are observed within the experimental resolution. In any case, despite the very close roughness values of 5.7 and 2.9 Å measured in samples A and C, respectively, very significant differences in their topography were found. Therefore, the AES results together with the AFM observations indicate that MgO does not wet completely the Fe bottom electrode when grown at 670 K, being porous when grown at RT. However, the annealing treatment of this MgO layer gives rise to a more compact, porous free, and continuous barrier.

In summary, we have reported an interface asymmetry in tunnel junction-like Fe/MgO/Fe(001) structures. AES depth profiling experiments show that both interfaces are spatially different, the MgO/Fe interface being broader than the Fe/MgO one, and also chemically, with the presence of a FeO interfacial layer in the MgO/Fe interface. This is due to the different fabrication procedure to obtain both interfaces. These results together with AFM measurements suggest the more likely presence of pinholes in the MgO barrier grown at 670 K as compared to that grown at low temperature and annealed at moderate temperatures.

This work was supported by the Spanish MCyT.

¹W. H. Butler, X. G. Zhang, T. C. Schulthess, and J. M. MacLaren, *Phys. Rev. B* **63**, 054416 (2001).

²J. Mathon, and A. Umerski, *Phys. Rev. B* **63**, 220403(R) (2001).

³M. Bowen, V. Cros, F. Petroff, A. Fert, C. Martinez Boubeta, J. L. Costa-Krämer, J. V. Anguita, A. Cebollada, F. Briones, J. M. de Teresa, L. Morellón, M. R. Ibarra, F. Güell, F. Peiró, and A. Cornet, *Appl. Phys. Lett.* **79**, 1655 (2001).

⁴E. Popova, J. Faure-Vincent, C. Tiusan, C. Bellouard, H. Fischer, M. Hehn, F. Montaigne, M. Alnot, S. Andrieu, A. Schuhl, E. Snocck, and V. da Costa V, *Appl. Phys. Lett.* **81**, 1035 (2002).

⁵J. Faure-Vincent, C. Tiusan, E. Jouguelet, F. Canet, M. Sajieddine, C. Bellouard, E. Popova, M. Hehn, F. Montaigne, and A. Schuhl, *Appl. Phys. Lett.* **82**, 4507 (2003).

⁶X. G. Zhang, W. H. Butler, and A. Bandyopadhyay, *Phys. Rev. B* **68**, 092402 (2003).

⁷H. L. Meyerheim, R. Popescu, J. Kirschner, N. Jedrecy, M. Sauvage-Simkin, B. Heinrich, and R. Pinchaux, *Phys. Rev. Lett.* **87**, 076102 (2001).

⁸H. L. Meyerheim, R. Popescu, N. Jedrecy, M. Vedpathak, M. Sauvage-Simkin, R. Pinchaux, B. Heinrich, and J. Kirschner, *Phys. Rev. B* **65**, 144433 (2002).

⁹H. Oh, S. B. Lee, J. Seo, H. G. Min, and J-S. Kim, *Appl. Phys. Lett.* **82**, 361 (2003).

¹⁰J. L. Vassant, A. Marty, B. Gilles, and C. Chatillon, *J. Cryst. Growth* **219**, 444 (2000).

¹¹C. Martinez Boubeta, E. Navarro, A. Cebollada, F. Briones, F. Peiró, and A. Cornet, *J. Cryst. Growth* **226**, 223 (2001).

¹²C. Martinez Boubeta, J. L. Costa-Krämer, and A. Cebollada *J. Phys.: Condens. Matter* **15**, R1123 (2003).

¹³S. Hofmann, in *Auger and X-ray Photoelectron Spectroscopy*, Practical Surface Analysis Vol. 1: edited by D. Briggs and M. P. Seah (Wiley, New York, 1990).

¹⁴E. V. Henrich, *Rep. Prog. Phys.* **48**, 1481 (1985).